Heat Treatment Optimization of Internal Tin Nb_3Sn Strands

Emanuela Barzi, Eric Gregory, and Tae Pyon

***Abstract*—The development of high critical current density (J_c) multifilamentary Nb_3Sn strands with low magnetization is important for many technological applications, including construction of high field accelerator magnets. To achieve this goal, strand R&D is actively pursued by Fermilab and IGC using the Internal Tin process. The J_c of a Nb_3Sn strand made with the Internal Tin technology depends on numerous factors, including Nb filament size and heat treatment cycle. Various heat treatments were applied to Nb_3Sn strands of different designs produced by IGC. The effect of filament size was studied both during the Nb_3Sn layer growth and after complete reaction. The resulting J_c's are presented, as well as SEM microscopy of strand sections.**

***Index Terms*—Critical current density, heat treatment, internal tin, subelement.**

I. Introduction

WITHIN the framework of an R&D program towards future accelerators, high field Nb_3Sn dipole magnets with nominal field above 11T are being developed at several National Labs. For a safe and reliable operation, the critical current density in the non-Cu section of the strand, J_c, that is needed at 4.2K and 12T to reach such fields is about 3000 A/mm^2. An accelerator magnet also needs excellent field uniformity. Reference [1] shows that even if the persistent current effect can be substantially reduced with passive corrections, this is possible only for superconductors with an effective filament diameter, d_{eff}, of less than 30-40 µm. The development of high J_c multifilamentary Nb_3Sn strands with low magnetization is therefore important for accelerator magnets.

The J_c of a Nb_3Sn strand made with the Internal Tin technology depends on numerous factors, including number and design of the strand subelements (SE), filament size, amount of Sn and of Nb in the non-Cu section, type of Nb-alloy used, Cu to non-Cu ratio, and heat treatment (HT) cycle. This paper addresses J_c sensitivity to strand design, filament size and HT. Various HT cycles were applied to several Nb_3Sn strands of different designs produced by IGC using the Internal Tin process. The effect on J_c was measured and strand sections were examined with SEM microscopy and chemical analyses.

Manuscript received September 17, 2000. This work was supported by the US Department of Energy.

E. Barzi is with Fermilab, Batavia, IL 60510 USA (telephone: 630-840-3446, e-mail: barzi@fnal.gov). E. Gregory and T. Pyon are with IGC-AS, Waterbury, CT 06704 USA (telephone: 203-753-5215).

II. The Experiment

A. Strand Description

The design parameters of the R&D Nb_3Sn strands that were used for this study are listed in Table I. The filament diameters were calculated from wire reduction. They were divided in two design groups, one with *Fine Filaments* (FF) and one with *Large Filaments* (LF). Some of these strands are described in more detail in [2].

B. Sample Preparation and Measurement Procedure

For this study, several sets of samples were prepared and tested. A different thermal cycle was used for each set to monitor the dependence of the strand superconducting properties on HT. These sets were heat treated in argon atmosphere according to the schedules shown in Table II. The samples to be used for I_c measurements were wound on grooved cylindrical barrels made of Ti-6Al-4V alloy [3]. After HT, voltage-current characteristics (VI) were measured

TABLE I
R&D Strand Parameters

Fine Filaments

ID	F1	F2	F3	F4
No. of SE	19	19	37	37
Split SE	N	N	N	N
Barrier	Round	Hex	Round	Hex
Sn, at. %	12.4	12.4	12.4	12.4
Nb, at. %	34.3	34.3	34.3	34.3
Strand diameter, mm	1.0 0.6 0.4	0.7 0.4	1.0 0.8 0.6 0.4	0.8
Filament size, µm	2.16 1.30 0.86	1.51 0.86	1.58 1.27 0.95 0.63	1.27
Cu fraction, %	38	38	38	38

Large Filaments

ID	ITER	L1	L2	L3	L4	L5	L6	L7
No. of SE	19	61	61	37	61	37	37	37
3-Split	N	Y	Y	Y	Y	Y	Y	N
Barrier	Round	Hex	Hex	Hex	Hex	Hex	Round	Round
Sn, at. %	10.1	10.8	13.4	14.1	15.1	15.1	17.3	17.6
Nb, at. %	20.4	29.4	29.0	30.5	29.6	29.6	32.6	35.9
Strand diameter, mm	1.0 0.7 0.5 0.3	1.0	1.0	1.0	1.0	0.8	1.0	1.0
Filament size, µm	5.2 3.7 2.6 1.6	4.8	4.7	6.3	4.9	5.3	6.2	6.2
Cu fr., %	58.7	38	46.5	46.5	47	42.5	38	38

TABLE II
HEAT TREATMENT STUDIES

Heat treatment No [a]		Step 1	Step 2	Step 3	Step 4	Total time, d
Temperature, °C	**1**	185	460	575	650	25
Duration, h		100	100	200	175	
Temperature, °C	**2**	185	460	575	650	28
Duration, h		100	100	200	250	
Temperature, °C	**3**	185	575	680		24
Duration, h		100	200	250		
Temperature, °C	**4**	575	650	680		20
Duration, h		200	175	75		
Temperature, °C	**5**	575	650			17
Duration, h		200	180			
Ramp rate, °C/h		6	8	10		
Temperature, °C	**6**	460	570	750		17.5
Duration, h		100	200	70		
Ramp rate, °C/h		6	8	10		
Temperature, °C	**7**	460	570	750		16
Duration, h		100	200	30		
Ramp rate, °C/h		6	25	25		
Temperature, °C	**8**	460	570	750		17
Duration, h		100	200	22		
Temperature, °C	**9**	575	750			10
Duration, h		200	18			
Temperature, °C	**10**	575	750			10
Duration, h		200	17			
Temperature, °C	**11**	575	700			13
Duration, h		200	90			
Temperature, °C	**12**	575	700			13
Duration, h		200	80			
Temperature, °C	**13**	575	700			12.5
Duration, h		200	70			
Temperature, °C	**14**	575	700			12
Duration, h		200	60			
Temperature, °C	**15**	575	700			11.5
Duration, h		200	50			
Temperature, °C	**16**	575	700			11
Duration, h		200	40			
Temperature, °C	**17**	575	700			11
Duration, h		200	30			
Temperature, °C	**18**	600	700			12
Duration, h		200	60			
Temperature, °C	**19**	575				9
Duration, h		200				

[a] Unless otherwise specified, the temperature ramp rate is 25°C/h.

in boiling He at 4.2 K, in a transverse magnetic field, B, up to 15 T. The I_c was determined from the VI curve using the $10^{-14}\Omega\cdot$m resistivity criterion. The relative directions of B and I were such as to generate an inward Lorentz force. Due to the latter and to the differential thermal contraction between sample and barrel, the specimen is subject to a tensile strain of up to 0.05% at 12 T and 4.2 K. This leads to a systematic error in the 3 to 5 % range on I_c [4]. The n-values were determined in the $V(I_c)$ to $10\cdot V(I_c)$ range by fitting the VI curve with the power law $V \sim I^n$. The estimated uncertainty of the I_c measurements at 4.2 K and 12 T is within ±1%.

III. TEST RESULTS AND DISCUSSION

A. First Observations

Preliminary HT studies involved several temperature steps for a time that was thought sufficient to carry out first Sn diffusion and homogenization in the Cu, next Sn reaction with the Nb and A15 phase formation. Fig. 1 shows results on I_c at 12 T for three different LF strands under HT-1 to 4. The effect of HT on I_c was well reproduced for all three designs. Here the following observations were made: 1) Increasing the time at 650°C to 250 h did not improve I_c; 2) Removing the lower temperature steps (*i.e.* steps below 500°C) did not reduce I_c.

Next HT-5 (final step at 650°C, no low temperature steps) and HT-6 to 10 (final step at 750°C, with and without a 460°C temperature step) were tried. Whereas the former HT produced a similar I_c or better than the previous multi-step HT's, the I_c obtained from HT-6 was about 30% lower. However, it was soon noticed that the I_c performance improved by decreasing the reaction time. As shown in Fig. 2 for two LF strands, reducing the time at 750°C from 70 down to 17 h improved I_c(12 T) by 20% or more. Also, SEM pictures of reacted filaments of strand L2 under HT-5 showed incomplete reaction. Over a large fraction of the strand, the filaments presented the pattern shown in Fig. 3 (left), where about 5 % of the cross sectional area is unreacted. This occurred after 180h at 650°C and is consistent with results of EDS analysis performed in [6]. On the contrary, only 17 h at 750°C (HT-10) were enough to complete filament reaction (see Fig. 3, right) throughout the whole strand. This was proven true also for HT-11 (90 h at 700°C, no low temperature steps). Therefore, besides requiring shorter times, higher temperature steps looked advantageous also in term of layer growth enhancement. Due to thermal constraints on the structural materials of the magnet, it was decided to pursue I_c optimization with 700°C as the highest HT temperature.

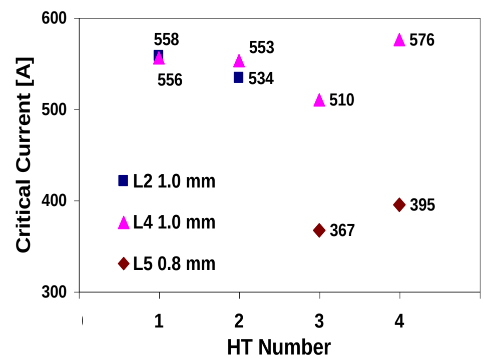

Fig. 1. I_c(12 T) vs. HT number (HT-1 to 4) for strands L2, L4 and L5. Shown on the plot are the I_c values in Amperes.

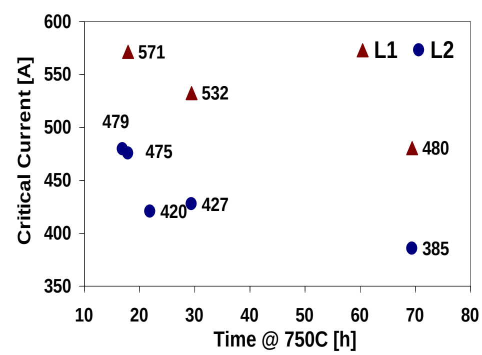

Fig. 2. I_c(12T) vs. HT time at 750°C for strands L1 and L2 under HT-6 to 10. Shown on the plot are the I_c values in Amperes.

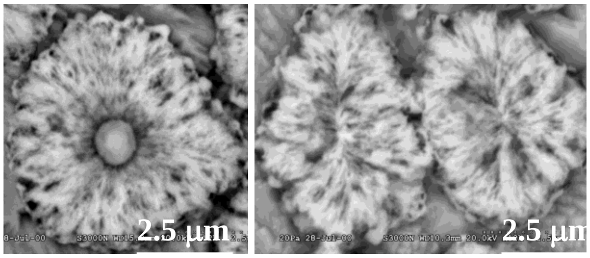

Fig. 3. SEM pictures of filaments in strand L2 after HT-5 (left) and after HT-10 (right).

B. HT Optimization

The time range that was explored at 700°C went from 90 h down to 30 h with HT-11 to 17. Note that only one step of 200 h at 575°C preceded the 700°C step. Fig. 4 shows the I_c results obtained at 12 T for two LF strands. The sensitivity of I_c to the time spent at 700°C appeared to be less significant with respect to that at 750°C. Also, HT-18 (*i.e.* with a first step at 600°C) produced a similar I_c as HT-14.

To measure the effect of time at the highest HT temperature on the J_c, HT-13, 15, and 17 (*i.e.* 70, 50 and 30 h at 700°C) were applied to several FF and LF strands. Figs. 5, 6, and 7 show the obtained J_c(12 T). Data points under 0 h at 700°C are associated to HT-19. It was noticed that within the FF set, the optimized times for F1 and F2 (19 SE designs) were in the 50 to 70 h range, whereas for F3 and F4 (37 SE designs) they were in the 40 to 50 h range. However, the J_c of the 0.4 mm F2 (*i.e.* very fine filaments) attained its peak after only 30 h. Within the LF set (all 37 and 61 SE designs, but ITER), the optimized times were also in the 40 to 50 h range.

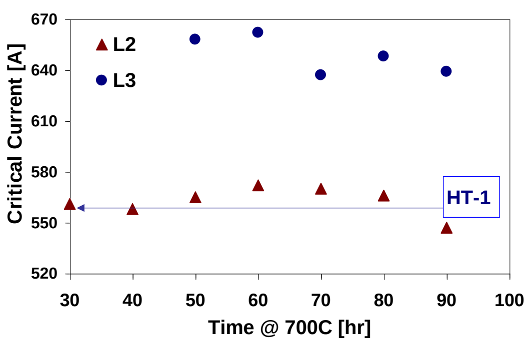

Fig. 4. I_c(12T) vs. HT time at 700°C for L2 and L3 under HT-11 to 17.

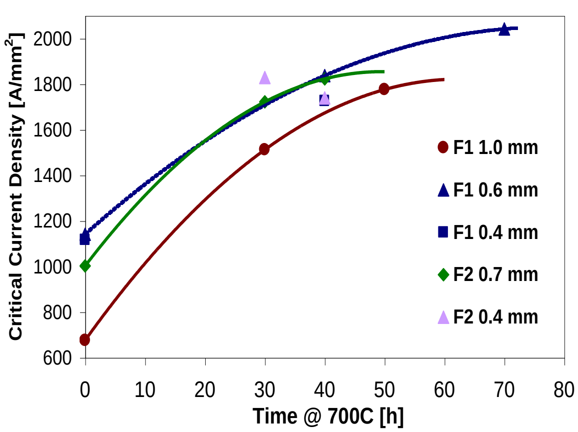

Fig. 5. J_c(12 T) vs. HT time at 700°C for F1 and F2 under HT-13, 15, 17, and 19.

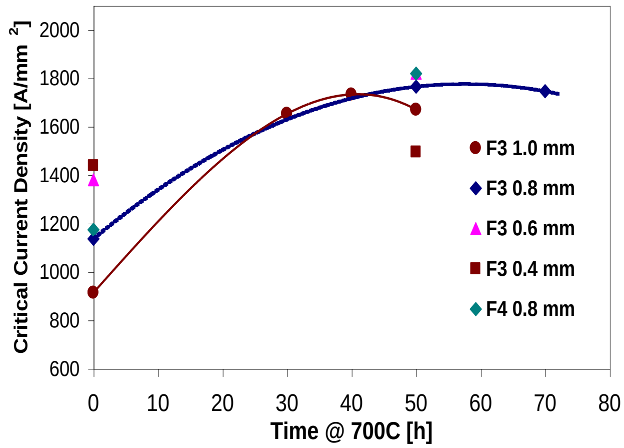

Fig. 6. J_c(12 T) vs. HT time at 700°C for F3 and F4 under HT-15, 17, 19.

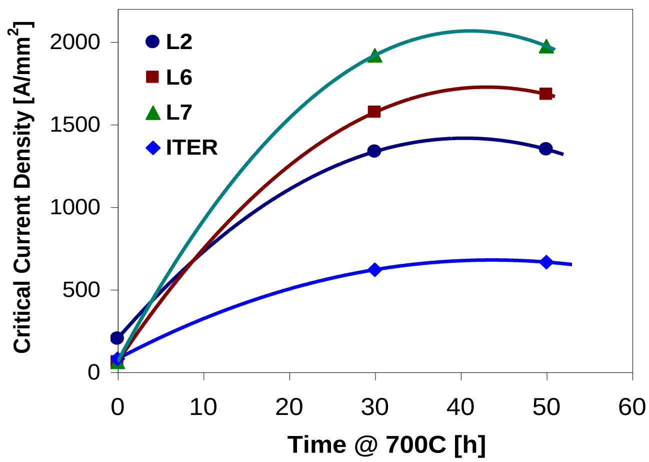

Fig. 7. J_c(12 T) vs. HT time at 700°C for LF strands under HT-15, 17, 19.

C. Effect on I_c of Filament Size

The effect of filament size (FS) on I_c performance was investigated both during the Nb_3Sn layer growth and after full reaction. Strand designs were chosen such as to cover the largest possible range of FS.

In order to better understand the process taking place during layer growth, strands of different designs were tested after being only partially reacted. As can be seen from Fig. 8 showing J_c(12 T) vs. FS after HT-19 (*i.e.* 200 h at 575°C), which provides only a partial reaction of the Nb, an exponential behavior is apparent for all strand designs. Data were fitted within each design and all gave a coefficient in the exponent of about -0.5 μm^{-1}. All fits but that for ITER gave an amplitude in the 2000 to 2200 A/mm^2 range. The highest J_c was greater than 1400 A/mm^2 and was obtained for the 0.4 mm F3. SEM microscopy was performed on a number of strands after HT-19, as shown in Figs. 9-11. The FF strands appear to have undergone a significant amount of reaction. The Nb_3Sn stoichiometry was checked also with EDS line scans. Figs. 9 and 10 show that for a given design, the Nb_3Sn layer thickness is the same for all strand sizes. However, the reacted thickness is larger for F3 (*i.e.* 37 SE) with respect to F1 (*i.e.* 19 SE). Although not shown in Figure, the 0.4 mm F3 sample was reacted throughout.

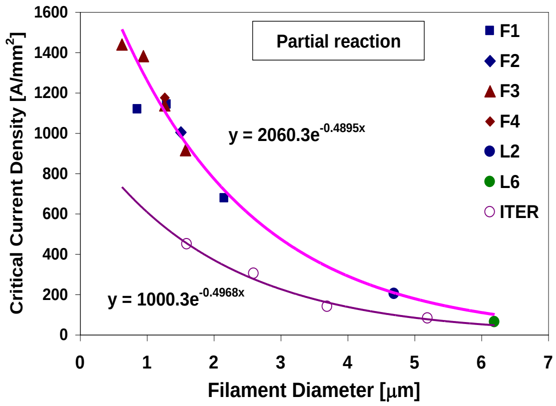

Fig. 8. J_c(12 T) as a function of FS for several strands after 200 h at 575°C.

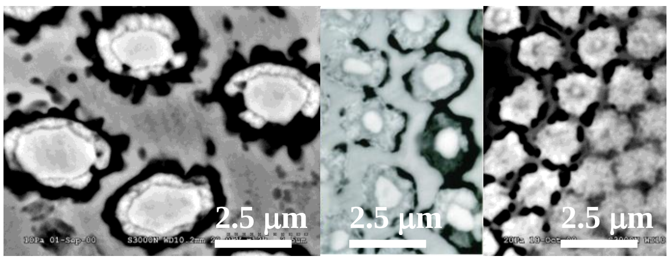

Fig. 9. SEM of F1, 1.0 mm (left), 0.6 mm (center), and 0.4 mm (right) under HT-19.

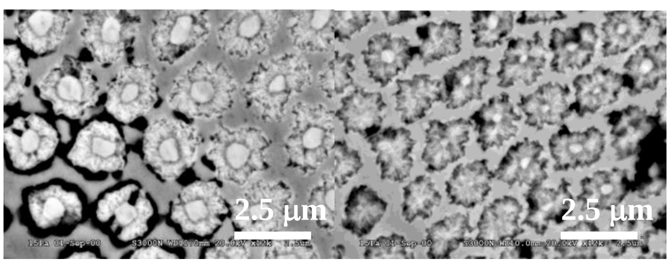

Fig. 10. SEM of F3, 1.0 mm (left), and 0.8 mm (right) under HT-19.

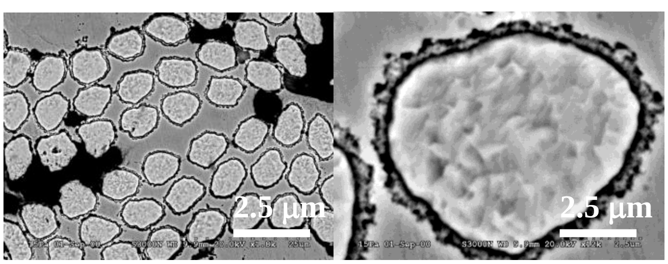

Fig. 11. SEM of L6, 1.0 mm under HT-19.

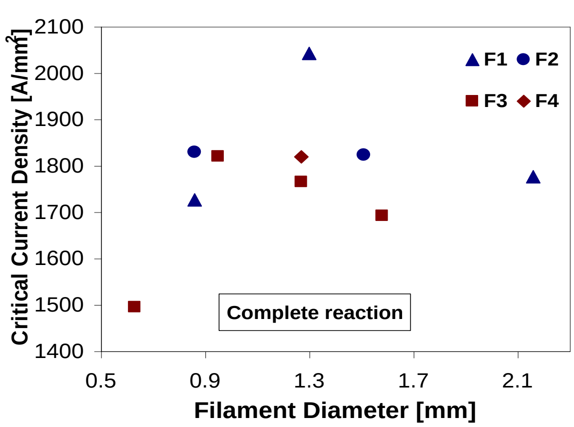

Fig. 12. Peak J_c(12 T) as a function of FS for fully reacted FF strands.

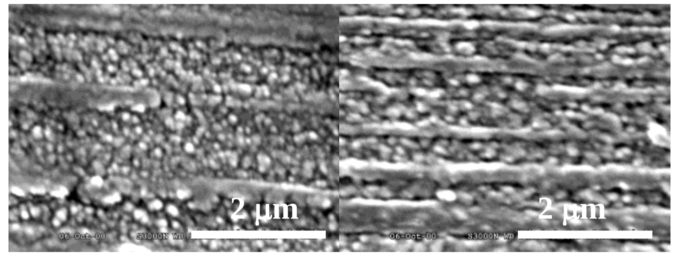

Fig. 13. SEM of longitudinal cross section of F3 after HT-19 (left), and after HT-15 (right).

After HT that led to full reaction of the Nb, the peak J_c(12T) obtained for each FF strand was plotted vs. FS in Fig. 12. The F1 and F3 data show that below a FS of about 1 to 1.3 µm, the peak J_c drops abruptly.

The longitudinal cross sections in Fig. 13 show that HT-19 at 575°C produces a grain size on the order of 100 nm. A HT that includes a second step of 50 h at 700°C causes the reacted grains to grow up to about 200 nm. Despite this the J_c increases significantly, suggesting that the phase or phases formed at 575°C undergo important changes at the higher temperature.

IV. Summary

A much shorter HT - 200 h at 575°C followed by 30 to 80 h at 700°C - has been used instead of the multi-step HT developed previously, with no degradation in I_c. However, in magnet manufacture care must be taken in the removal of some of the low temperature steps unless they can be replaced by a slow overall ramp rate. In this application a temperature of 700°C was chosen as the highest one. This was practical in wind and react magnet manufacture.

The effect on J_c and the extent to which the filaments are reacted after 200 h at 575°C only were examined in materials with different filament diameters. An exponential relationship between J_c and filament diameter was observed. A J_c higher than 1400 A/mm^2 at 12T could be obtained with filament diameters of less than 1 µm. However, after completion of the reaction at 700°C, the J_c dropped for a FS below about 1 µm.

A HT with a second step of 50 h at 700°C doubled the size of the grains of material reacted at 575°C. A HT of 70 h at 700°C raised the J_c to 2000 A/mm^2 at 12 T. Such significant increase in J_c suggests that the phase formed at 575°C undergoes important changes at the higher temperature.

Acknowledgment

E. B. thanks Tom Wokas, whose precious work made this paper possible.

References

[1] V.V. Kashikhin and A.V. Zlobin, “Correction of the persistent current effect in Nb_3Sn dipole magnets”, this Conference Proceedings, submitted for publication.

[2] T. Pyon and E. Gregory, “Nb_3Sn Conductors for High Energy Physics and Fusion Applications”, this Conference Proceedings, submitted for publication.

[3] L. F. Goodrich et al., “Superconductor critical current standards for fusion applications”, NISTIR 5027, NIST.

[4] E. Barzi et al., “Error analysis of short sample Jc measurements at the Short Sample Test Facility”, Fermilab, TD-98-055[1], Sept. 1998.

[1] Accessible from the web: http://tdserver1.fnal.gov/tdlibry/TD-Notes/.